Dependence of fusion on isospin dynamics

K. Godbey,[1,*] A.S. Umar,[1,†] and C. Simenel[2,‡]

[1]*Department of Physics and Astronomy, Vanderbilt University, Nashville, TN 37235, USA*
[2]*Department of Nuclear Physics, Research School of Physics and Engineering, The Australian National University, Canberra ACT 2601, Australia*

(Dated: December 9, 2016)

We introduce a new microscopic approach to calculate the dependence of fusion barriers and cross-sections on isospin dynamics. The method is based on the time-dependent Hartree-Fock theory and the isoscalar and isovector properties of the energy density functional (EDF). The contribution to the fusion barriers originating from the isoscalar and isovector parts of the EDF is calculated. It is shown that for non-symmetric systems the isovector dynamics influence the sub-barrier fusion cross-sections. For most systems this results in an enhancement of the sub-barrier cross-sections, while for others we observe differing degrees of hindrance. We use this approach to provide an explanation of recently measured fusion cross sections which show a enhancement at low $E_{\rm c.m.}$ energies for the system ^{40}Ca+^{132}Sn as compared to the more neutron-rich system ^{48}Ca+^{132}Sn, and discuss the dependence of sub-barrier fusion cross-sections on transfer.

One of the major open questions in fusion reactions of exotic neutron-rich nuclei is the dependence of the fusion cross section on the neutron excess, or equivalently on the total isospin quantum number $T_z = (Z-N)/2$. This is a timely subject given the expected availability of increasingly exotic beams at rare isotope facilities [1]. The influence of isospin dynamics on fusion is also one of the key questions pertaining to the production of superheavy elements using neutron rich nuclei [2]. Besides being a fundamental nuclear structure and reaction question, the answer to this inquiry is also vital to our understanding of the nuclear equation of state (EOS) and symmetry energy [3]. The EOS plays a key role in elucidating the structure of exotic nuclei [4], the dynamics of heavy ion collisions [5,6], the composition of neutron stars [7–10], and the mechanism of core-collapse supernovae [11–13]. The influence of isospin flow during heavy-ion reaction is usually discussed in term of the (N/Z) asymmetry of the target and projectile or the Q-values for nucleon transfer.

The presence of positive $Q-$value transfer channels has been shown to enhance sub-barrier fusion in various systems [14]. However, what affects the magnitude of this enhancement is still actively debated [15–19]. In particular, recent experiments carried out with radioactive ^{132}Sn beams and with stable ^{124}Sn beams on ^{40,48}Ca [17] and ^{58,64}Ni [15] targets have shown that the enhancement is observed at much lower cross-sections in the heavier (Ni+Sn) systems [18] than in the lighter (Ca+Sn) ones. Various possible effects have been invoked to explain these observations [19], such as a larger role of dissipation due to the increase of the charge product Z_1Z_2 of the collision partners [20–22]. It is also known that for systems with $Z_1Z_2 \gtrsim 1600$, the so-called quasi-fission, where the nuclei re-separate after a significant mass transfer, strongly hinders fusion [23].

The effect of neutron transfer on fusion is traditionally described within the coupled-channels (CC) method [24–26] and models incorporating intermediate neutron rearrangements [27–29]. These approaches, however, model the transfer process on a schematic way and they require nuclear data which are often unknown for exotic nuclei. New approaches are then needed to describe realistically the effect of both proton and neutron transfers on fusion of stable and exotic nuclei. In particular, dissipation induced by transfer should be properly accounted for.

Here, we take a first step toward this ambitious theoretical program by investigating the overall effect of isospin dynamics induced mostly by neutron and/or proton transfer in collisions of asymmetric systems [30–39]. In particular, we address the impact of isospin dynamics on fusion barriers and cross-sections using the microscopic time-dependent Hartree-Fock (TDHF) theory [40,41] together with the density-constrained TDHF (DC-TDHF) method for calculating fusion barriers [42]. This choice is motivated by the fact that the TDHF approach has been used to successfully describe multinucleon transfer [43–47], as well as strongly damped reactions such as deep-inelastic collisions [48,49] and quasi-fission [50–52], without relying on an *a priori* knowledge of the structure of the reactants. Therefore, these microscopic dynamical calculations incorporate the fundamental mechanisms which are relevant for a realistic description of the effect of transfer on fusion, including with exotic beams. As a first application, various systems from Ca+Ca to Ca+Sn are considered.

In the TDHF approximation the many-body wavefunction is replaced by a single Slater determinant and this form is preserved at all times, implying that two-body correlations are neglected. In this limit, the variation of the time-dependent action with respect to the single-particle states, ϕ_λ^*, yields the most probable time-dependent path in the multi-dimensional space-time phase space represented as a set of coupled, non-linear, self-consistent initial value equations for the single-particle states

$$h(\{\phi_\mu\})\,\phi_\lambda(r,t) = i\hbar\frac{\partial}{\partial t}\phi_\lambda(r,t) \quad (\lambda = 1,...,A)\,, \qquad (1)$$

where h is the HF single-particle Hamiltonian. These are the fully microscopic time-dependent Hartree-Fock equations.

* kyle.s.godbey@vanderbilt.edu
† umar@compsci.cas.vanderbilt.edu
‡ cedric.simenel@anu.edu.au

Almost all TDHF calculations employ the Skyrme EDF, which allows the total energy of the system to be represented as an integral of the energy density $\mathscr{H}(\mathbf{r})$ [53]

$$E = \int d^3\mathbf{r}\mathscr{H}(\mathbf{r}), \tag{2}$$

which includes the kinetic, isoscalar, isovector, and Coulomb terms [54]:

$$\mathscr{H}(\mathbf{r}) = \frac{\hbar^2}{2m}\tau_0 + \mathscr{H}_0(\mathbf{r}) + \mathscr{H}_1(\mathbf{r}) + \mathscr{H}_C(\mathbf{r}). \tag{3}$$

In particular,

$$\mathscr{H}_{\rm I}(\mathbf{r}) = C_{\rm I}^{\rho}\rho_{\rm I}^2 + C_{\rm I}^{s}\mathbf{s}_{\rm I}^2 + C_{\rm I}^{\Delta\rho}\rho_{\rm I}\Delta\rho_{\rm I} + C_{\rm I}^{\Delta s}\mathbf{s}_{\rm I}\cdot\Delta\mathbf{s}_{\rm I} + C_{\rm I}^{\tau}\left(\rho_{\rm I}\tau_{\rm I} - \mathbf{j}_{\rm I}^2\right) + C_{\rm I}^{T}\left(\mathbf{s}_{\rm I}\cdot\mathbf{T}_{\rm I} - \overleftrightarrow{J}_{\rm I}^2\right) + C_{\rm I}^{\nabla J}\left(\rho_{\rm I}\nabla\cdot\mathbf{J}_{\rm I} + \mathbf{s}_{\rm I}\cdot(\nabla\times\mathbf{j}_{\rm I})\right), \tag{4}$$

where we have used the gauge invariant form suitable for time-dependent calculations. The isospin index $\mathrm{I} = 0, 1$ for isoscalar and isovector energy densities, respectively. The most common choice of Skyrme EDF restricts the density dependence of the coupling constants to the $C_{\rm I}^{\rho}$ and $C_{\rm I}^{s}$ terms only. These density dependent coefficients contribute to the coupling of isoscalar and isovector fields in the Hartree-Fock Hamiltonian. The isoscalar (isovector) energy density, $\mathscr{H}_0(\mathbf{r})$ ($\mathscr{H}_1(\mathbf{r})$), depends on the isoscalar (isovector) particle density, $\rho_0 = \rho_n + \rho_p$ ($\rho_1 = \rho_n - \rho_p$), with analogous expressions for other densities and currents. Values of the coupling coefficients as well as their relation to the alternative parametrizations of the Skyrme EDF can be found in [54].

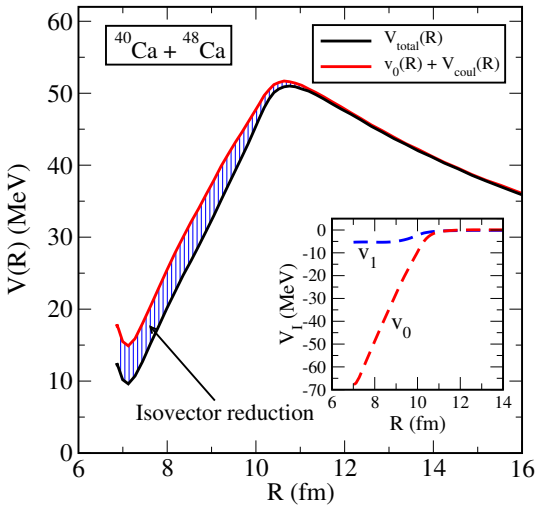

FIG. 1. (Color online) For the ^{40}Ca+^{48}Ca system; Total and isoscalar DC-TDHF potentials. The shaded region corresponds to the reduction originating from the isovector contribution to the energy density. The insert shows the isoscalar and isovector contributions to the interaction barrier without the Coulomb potential. The TDHF collision energy was $E_{\rm c.m.} = 55$ MeV.

The above form of the EDF is more suitable for studying the isospin dependence of nuclear properties and have been employed in nuclear structure studies [54]. In the same spirit we can utilize this approach to study isospin dependent effects in nuclear reactions microscopically. In particular, the density-constrained time-dependent Hartree-Fock (DC-TDHF) method [42] can be employed to study isospin effects on fusion barriers and fusion cross-sections. The DC-TDHF approach calculates the nucleus-nucleus potentials $V(R)$ directly from TDHF dynamics and has been used to calculate fusion cross-sections for a wide range of reactions [55–61]. The basic idea of this approach is the following: At certain times t or, equivalently, at certain internuclear distances $R(t)$, a static energy minimization is performed while constraining the proton and neutron densities to be equal to the instantaneous TDHF densities. We refer to the minimized energy as the "density constrained energy" $E_{\rm DC}(R)$. The ion-ion interaction potential $V(R)$ is obtained by subtracting the constant binding energies $E_{\rm A_1}$ and $E_{\rm A_2}$ of the two individual nuclei

$$V(R) = E_{\rm DC}(R) - E_{\rm A_1} - E_{\rm A_2}\ . \tag{5}$$

The calculated ion-ion interaction barriers contain all of the dynamical changes in the nuclear density during the TDHF time-evolution in a self-consistent manner. As a consequence of the dynamics the DC-TDHF potential is energy dependent [55]. Using the decomposition of the Skyrme EDF into isoscalar and isovector parts [Eq. (4)], we can re-write this potential as

$$V(R) = \sum_{\rm I=0,1} v_{\rm I}(R) + V_C(R), \tag{6}$$

where $v_{\rm I}(R)$ denotes the potential computed by using the isoscalar and isovector parts of the Skyrme EDF given in Eq. (3) in Eq. (5). The Coulomb potential is also calculated via Eq. (5) using the Coulomb energy density.

We have used the DC-TDHF approach to study fusion barriers for a number of systems. Calculations were done in a three-dimensional Cartesian geometry with no symmetry assumptions [62] and using the Skyrme SLy4 EDF [63]. The three-dimensional Poisson equation for the Coulomb potential is solved by using Fast-Fourier Transform techniques and the Slater approximation is used for the Coulomb exchange term. The box size used for all the calculations was chosen to be $60\times30\times30$ fm^3, with a mesh spacing of 1.0 fm in all directions. These values provide very accurate results due to the employment of sophisticated discretization techniques [64].

In Fig. 1 we show the total and isoscalar fusion barriers (both including the Coulomb contribution) for the ^{40}Ca+^{48}Ca system at $E_{\rm c.m.} = 55$ MeV. For the Ca+Ca systems the energy dependence is relatively weak [55,65,66]. The reduction of the isoscalar barrier is due to the isovector contribution. It is

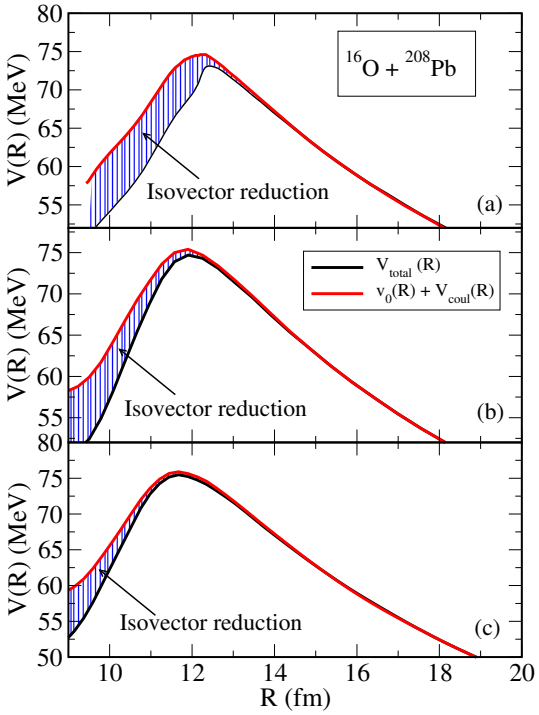

FIG. 2. (Color online) For the ^{16}O+^{208}Pb system; (a) Total and isoscalar DC-TDHF potentials at $E_{\rm c.m.} = 75$ MeV. The shaded region corresponds to the reduction originating from the isovector contribution to the energy density. (b) Same as in (a) except for $E_{\rm c.m.} = 90$ MeV. (c) Same as in (a) except for $E_{\rm c.m.} = 120$ MeV.

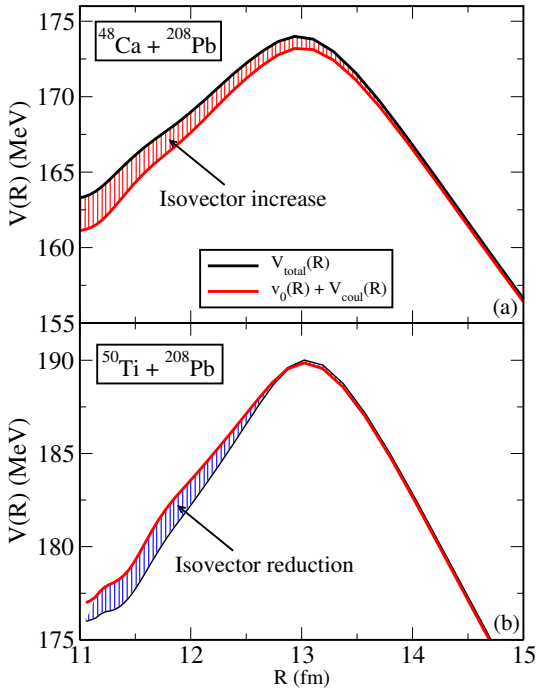

FIG. 3. (Color online) Isoscalar and isovector breakdown of the potential barrier for two systems at the same $E_{\rm c.m.}/V_B = 1.065$; (a) ^{48}Ca+^{208}Pb. The shaded region corresponds to the increase originating from the isovector contribution to the energy density. (b) Same as in (a) except ^{50}Ti+^{208}Pb. The shaded region corresponds to the decrease originating from the isovector contribution to the energy density.

evident that the isovector dynamics results in the narrowing of the fusion barrier, thus resulting in an enhancement of the sub-barrier fusion cross-sections. The insert in Fig. 1 shows the isovector and isoscalar components without the Coulomb contribution. We have also calculated fusion barriers for the ^{40}Ca+^{40}Ca and ^{48}Ca+^{48}Ca systems, where the isovector contribution is zero as expected from symmetry. Irrespective of its isovector/isoscalar nature, the DC-TDHF potential is a way to represent the potential felt by the system at a given time. The relation between time and distance between the fragments then allow to represent the potential in the traditional manner, i.e., as a function of the internuclear distance. The fact that the isovector reduction occurs essentially inside the barrier indicates that the proton and neutron flows become larger for stronger overlap occurring in the later stage of fusion.

As an example of a more asymmetric system we performed calculations for the ^{16}O+^{208}Pb system at $E_{\rm c.m.} = 75$ MeV. Results are shown in Fig. 2(a). Here we see a substantial enhancement of sub-barrier fusion due to the isovector dynamics. For this system we have performed further calculations at c.m. energies of 90 MeV and 120 MeV shown in Fig. 2(b-c). As the beam energy increases, the relative contribution from the isovector component to the total barrier decreases, while the overall barrier height increases with increasing energy. At TDHF energies much higher than the barrier height the total barriers approaches the frozen density barrier [55,66] due to the inability of the system to rearrange at that time-scale at which time the isovector contribution vanishes as well. Next, we have calculated isoscalar and isovector breakdown of the potential barrier for two systems at the same $E_{\rm c.m.}/V_B = 1.065$ as shown in Fig. 3(a,b) for; ^{48}Ca+^{208}Pb system where the shaded region corresponds to the increase in the barrier originating from the isovector contribution to the energy density, and for the ^{50}Ti+^{208}Pb system where the shaded region corresponds to the decrease in the barrier originating from the isovector contribution to the energy density. The above results demonstrate the influence of isovector dynamics on typical fusion barriers.

We next look at Ca+Sn reactions. The experimental observation of a sub-barrier fusion enhancement in the system ^{40}Ca+^{132}Sn as compared to more neutron-rich system ^{48}Ca+^{132}Sn was the subject of a previous DC-TDHF study [67], where it was shown that the fusion barriers for the two systems have essentially the same height but the fusion barrier for the ^{48}Ca+^{132}Sn system was much wider than that for the ^{40}Ca+^{132}Sn system. We see in Fig. 4(a) a strong reduction of the isoscalar barrier due to the isovector contribution. This behavior is similar to that of the previous two systems albeit the isovector reduction is somewhat larger as shown in the insert of Fig. 4(a). We then performed the same calculation for the ^{48}Ca+^{132}Sn system as shown in Fig. 4(b). The startling result is the vanishing of the isovector contribution. With no isovector reduction the fusion barrier for this system is much

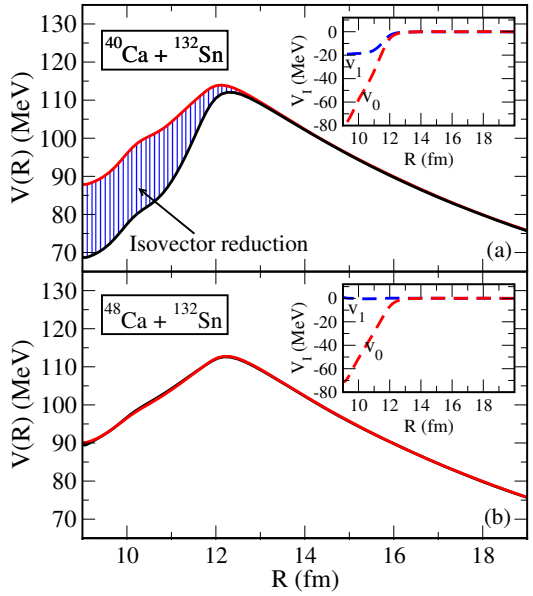

FIG. 4. (Color online) For (a) ^{40}Ca+^{132}Sn, (b) ^{48}Ca+^{132}Sn systems; Total and isoscalar DC-TDHF potentials. In (a) the blue shaded region corresponds to the reduction originating from the isovector contribution. In (b) we see no isovector effect. (c) the isovector effect is reversed causing hindrance as shown by the red shaded region. The inserts show the isoscalar and isovector contributions to the interaction barrier without the Coulomb potential. The TDHF collision energy was $E_{\rm c.m.} = 120$ MeV.

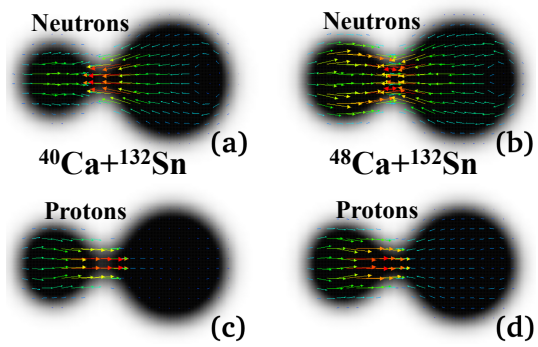

FIG. 5. (Color online) Neutron and proton current vectors in ^{40,48}Ca+^{132}Sn at $E_{\rm c.m.} = 120$ MeV and at a separation $R = 11.5$ fm between the fragments.

wider than that for the ^{40}Ca+^{132}Sn system for which substantial reduction occurs. The absence of the isovector component for the ^{48}Ca+^{132}Sn system could be a reflection of the negative $Q-$values for neutron pickup. This is the first direct observation of this phenomena in microscopic calculations.

This may also explain why for the ^{48}Ca+^{132}Sn system simply considering the 2^+ and 3^- excitations of the target and projectile in coupled-channel calculations is able to reproduce the sub-barrier fusion cross-sections, whereas doing the same for the ^{40}Ca+^{132}Sn system grossly under-predicts the cross-sections. In Ref. [17], this was attributed to transfer which manifests itself in the isovector dynamics. In Fig. 4(c) we have also calculated the potential barriers for the theoretical ^{54}Ca+^{132}Sn reaction. Here, we see that the influence of the isovector component is reversed, as indicated by the shaded region. This reversal leads to the widening of the potential barrier, further hindering sub-barrier fusion.

In all the studied systems, we observe an isovector reduction in the presence of positive $Q-$values for transfer channels. This can be understood from the $C_{\rm I}^{\rho}\rho_{\rm I}^2$ term in Eq. (3) which quantitatively dominates. When an isospin equilibration occurs (driven by positive $Q-$values), the $I = 1$ contribution gets reduced as $(\rho_p - \rho_n)^2$ decreases in each fragment and $C_{\rm I}^{\rho}$ is positive. This also explains why, in systems with only negative Q-values, the isovector contribution to the potential vanishes. In very few cases, such as for the theoretical ^{54}Ca+^{132}Sn reaction, we even found an increase of the potential which is attributed to more complex density dependencies of H_1 in Eq. (3).

In order to investigate the role of transfer in more detail we have plotted in Fig. 5 the microscopic TDHF neutron and proton currents for ^{40,48}Ca+^{132}Sn at $E_{\rm c.m.} = 120$ MeV and at the nuclear separation $R = 11.5$ fm, which is slightly inside the barrier but still corresponds to an early stage of the reaction. In ^{40}Ca+^{132}Sn, neutrons flow from Sn to Ca (Fig. 5a) and protons from Ca to Sn (Fig. 5c), compatible with the fact that there are many positive $Q-$value channels for these transfers to occur. For ^{48}Ca+^{132}Sn, which has no positive $Q-$value transfer channel, we observe a convergence of neutrons towards the neck (Fig. 5b), which is what we would expect in the fusion process. This is also what is observed for protons in (Fig. 5d), although there is a larger displacement of protons from Ca towards the neutron-rich neck. As a result, the isovector current density in the neck region is an order of magnitude lower for the ^{48}Ca+^{132}Sn system in comparison to the ^{40}Ca+^{132}Sn. This is the primary cause for the disappearance

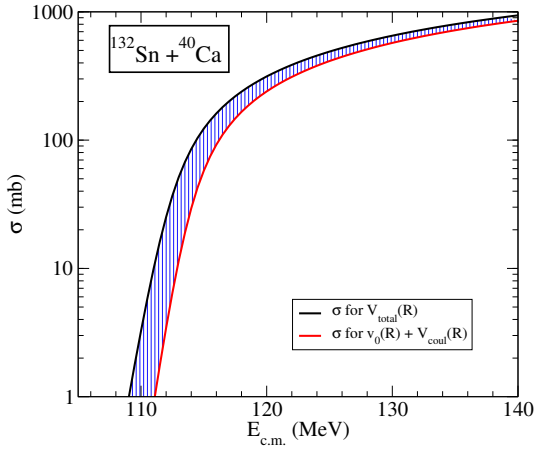

FIG. 6. (Color online) Fusion cross-section in ^{40}Ca+^{132}Sn calculated with (black line) and without (red line) isovector reduction, using the potentials of Fig. 4a.

of the isovector contribution to the barrier.

Finally, the impact of the isovector contribution to the fusion dynamics is shown in Fig. 6, where fusion cross-sections have been computed from the DC-TDHF potentials of Fig. 4a.

The effect of the isovector reduction is particularly visible at sub-barrier energies where an enhancement of the fusion cross-sections by about an order of magnitude is observed. To our knowledge, this is the first microscopic evidence of the enhancement of fusion due to coupling to transfer channels.

In summary, we have developed a microscopic approach to study the effect of isospin dynamics on fusion barriers. We have shown that for most systems isovector dynamics results in the thinning of the barrier thus enhancing the sub-barrier fusion cross-sections. The isovector reduction effect vanishes for symmetric systems as well as the ^{48}Ca+^{132}Sn system for which neutron pickup $Q-$values are all negative. These results provide a quantitative measure for the importance of transfer for sub-barrier fusion reactions. Furthermore, they elucidate the non-trivial dependence of sub-barrier fusion for neutron-rich systems and illustrate the importance of dynamical microscopic models that incorporate the nuclear structure and reactions on the same footing.

We thank K. Vo-Phuoc for useful discussions regarding the Ca+Sn systems. This work has been supported by the U.S. Department of Energy under grant No. DE-SC0013847 with Vanderbilt University and by the Australian Research Council Grant No. FT120100760.

[1] A. B. Balantekin, J. Carlson, D. J. Dean, G. M. Fuller, R. J. Furnstahl, M. Hjorth-Jensen, R. V. F. Janssens, B.-A. Li, W. Nazarewicz, F. M. Nunes, W. E. Ormand, S. Reddy, and B. M. Sherrill, Mod. Phys. Lett. A **29**, 1430010 (2014).
[2] W. Loveland, Phys. Rev. C **76**, 014612 (2007).
[3] B.-A. Li, Àngels. Ramos, G. Verde, and I. Vidaña, Eur. Phys. J. A **50**, 1 (2014).
[4] W.-C. Chen and J. Piekarewicz, Phys. Lett. B **748**, 284 (2015).
[5] P. Danielewicz, R. Lacey, and W. G. Lynch, Science **298**, 1592 (2002).
[6] M. B. Tsang, Y. Zhang, P. Danielewicz, M. Famiano, Z. Li, W. G. Lynch, and A. W. Steiner, Phys. Rev. Lett. **102**, 122701 (2009).
[7] P. Haensel and J. L. Zdunik, Astron. Astrophys. **229**, 117 (1990).
[8] N. Chamel and P. Haensel, Living Rev. Relat. **11**, 10 (2008).
[9] C. J. Horowitz, M. A. Pérez-García, and J. Piekarewicz, Phys. Rev. C **69**, 045804 (2004).
[10] R. Utama, J. Piekarewicz, and H. B. Prosper, Phys. Rev. C **93**, 014311 (2016).
[11] P. Bonche and D. Vautherin, Nucl. Phys. A **372**, 496 (1981).
[12] G. Watanabe, H. Sonoda, T. Maruyama, K. Sato, K. Yasuoka, and T. Ebisuzaki, Phys. Rev. Lett. **103**, 121101 (2009).
[13] G. Shen, C. J. Horowitz, and S. Teige, Phys. Rev. C **83**, 035802 (2011).
[14] C. L. Jiang, K. E. Rehm, B. B. Back, H. Esbensen, R. V. F. Janssens, A. M. Stefanini, and G. Montagnoli, Phys. Rev. C **89**, 051603(R) (2014).
[15] Z. Kohley, J. F. Liang, D. Shapira, R. L. Varner, C. J. Gross, J. M. Allmond, A. L. Caraley, E. A. Coello, F. Favela, K. Lagergren, and P. E. Mueller, Phys. Rev. Lett. **107**, 202701 (2011).
[16] Z. Kohley, J. F. Liang, D. Shapira, C. J. Gross, R. L. Varner, J. M. Allmond, J. J. Kolata, P. E. Mueller, and A. Roberts, Phys. Rev. C **87**, 064612 (2013).
[17] J. J. Kolata, A. Roberts, A. M. Howard, D. Shapira, J. F. Liang, C. J. Gross, R. L. Varner, Z. Kohley, A. N. Villano, H. Amro, W. Loveland, and E. Chavez, Phys. Rev. C **85**, 054603 (2012).
[18] C. L. Jiang, A. M. Stefanini, H. Esbensen, K. E. Rehm, S. Almaraz-Calderon, M. L. Avila, B. B. Back, D. Bourgin, L. Corradi, S. Courtin, E. Fioretto, F. Galtarossa, A. Goasduff, F. Haas, M. M. Mazzocco, D. Montanari, G. Montagnoli, T. Mijatovic, R. Sagaidak, D. Santiago-Gonzalez, F. Scarlassara, E. E. Strano, and S. Szilner, Phys. Rev. C **91**, 044602 (2015).
[19] J. F. Liang, J. M. Allmond, C. J. Gross, P. E. Mueller, D. Shapira, R. L. Varner, M. Dasgupta, D. J. Hinde, C. Simenel, E. Williams, K. Vo–Phuoc, M. L. Brown, I. P. Carter, M. Evers, D. H. Luong, T. Ebadi, and A. Wakhle, Phys. Rev. C **94**, 024616 (2016).
[20] F. L. H. Wolfs, Phys. Rev. C **36**, 1379 (1987).
[21] M. Evers, M. Dasgupta, D. J. Hinde, D. H. Luong, R. Rafiei, R. du Rietz, and C. Simenel, Phys. Rev. C **84**, 054614 (2011).
[22] D. C. Rafferty, M. Dasgupta, D. J. Hinde, C. Simenel, E. C. Simpson, E. Williams, I. P. Carter, K. J. Cook, D. H. Luong, S. D. McNeil, K. Ramachandran, K. Vo-Phuoc, and A. Wakhle, Phys. Rev. C **94**, 024607 (2016).
[23] J. Töke, R. Bock, G. X. Dai, A. Gobbi, S. Gralla, K. D. Hildenbrand, J. Kuzminski, W. F. J. Müller, A. Olmi, H. Stelzer, B. B. Back, and S. Bjørnholm, Nucl. Phys. A **440**, 327 (1985).
[24] N. Rowley, I. J. Thompson, and M. A. Nagarajan, Phys. Lett. B **282**, 276 (1992).
[25] H. Esbensen, C. L. Jiang, and K. E. Rehm, Phys. Rev. C **57**, 2401 (1998).
[26] Kouichi Hagino and Noboru Takigawa, Prog. Theo. Phys. **128**, 1001 (2012).
[27] V. I. Zagrebaev, Phys. Rev. C **67**, 061601 (2003).
[28] V. I. Zagrebaev, V. V. Samarin, and W. Greiner, Phys. Rev. C **75**, 035809 (2007).
[29] A. V. Karpov, V. A. Rachkov, and V. V. Samarin, Phys. Rev. C **92**, 064603 (2015).
[30] C. H. Dasso, S. Landowne, and A. Winther, Nucl. Phys. A **432**, 495 (1985).
[31] Ph. Chomaz, M. Di Toro, and A. Smerzi, Nucl. Phys. A **563**, 509 (1993).
[32] V. Baran, M. Colonna, M. Di Toro, A. Guarnera, and A. Smerzi, Nucl. Phys. A **600**, 111 (1996).
[33] V. Baran, D. M. Brink, M. Colonna, and M. Di Toro, Phys. Rev. Lett. **87**, 182501 (2001).
[34] C. Simenel, P. Chomaz, and G. de France, Phys. Rev. Lett. **86**, 2971 (2001).
[35] V. Baran, M. Colonna, V. Greco, and M. Di Toro, Phys. Rep. **410**, 335 (2005).
[36] C. Simenel, P. Chomaz, and G. de France, Phys. Rev. C **76**, 024609 (2007).
[37] V. Baran, C. Rizzo, M. Colonna, M. Di Toro, and D. Pierroutsakou, Phys. Rev. C **79**, 021603 (2009).
[38] V. E. Oberacker, A. S. Umar, J. A. Maruhn, and P.-G. Reinhard, Phys. Rev. C **85**, 034609 (2012).
[39] A. S. Umar, V. E. Oberacker, and J. A. Maruhn, Eur. Phys. J. A **37**, 245 (2008).
[40] J. W. Negele, Rev. Mod. Phys. **54**, 913 (1982).
[41] C. Simenel, Eur. Phys. J. A **48**, 152 (2012).

[42] A. S. Umar and V. E. Oberacker, Phys. Rev. C **74**, 021601 (2006).
[43] C. Simenel, Phys. Rev. Lett. **105**, 192701 (2010).
[44] C. Simenel, D. J. Hinde, R. du Rietz, M. Dasgupta, M. Evers, C. J. Lin, D. H. Luong, and A. Wakhle, Phys. Lett. B **710**, 607 (2012).
[45] Kazuyuki Sekizawa and Kazuhiro Yabana, Phys. Rev. C **88**, 014614 (2013).
[46] G. Scamps and D. Lacroix, Phys. Rev. C **87**, 014605 (2013).
[47] D. Bourgin, C. Simenel, S. Courtin, and F. Haas, Phys. Rev. C **93**, 034604 (2016).
[48] S. E. Koonin, K. T. R. Davies, V. Maruhn-Rezwani, H. Feldmeier, S. J. Krieger, and J. W. Negele, Phys. Rev. C **15**, 1359 (1977).
[49] C. Simenel, Phys. Rev. Lett. **106**, 112502 (2011).
[50] A. Wakhle, C. Simenel, D. J. Hinde, M. Dasgupta, M. Evers, D. H. Luong, R. du Rietz, and E. Williams, Phys. Rev. Lett. **113**, 182502 (2014).
[51] A. S. Umar, V. E. Oberacker, and C. Simenel, Phys. Rev. C **92**, 024621 (2015).
[52] A. S. Umar, V. E. Oberacker, and C. Simenel, Phys. Rev. C **94**, 024605 (2016).
[53] Y. M. Engel, D. M. Brink, K. Goeke, S. J. Krieger, and D. Vautherin, Nucl. Phys. A **249**, 215 (1975).
[54] J. Dobaczewski and J. Dudek, Phys. Rev. C **52**, 1827 (1995).
[55] A. S. Umar, C. Simenel, and V. E. Oberacker, Phys. Rev. C **89**, 034611 (2014).
[56] C. Simenel, R. Keser, A. S. Umar, and V. E. Oberacker, Phys. Rev. C **88**, 024617 (2013).
[57] A. S. Umar, V. E. Oberacker, and C. J. Horowitz, Phys. Rev. C **85**, 055801 (2012).
[58] A. S. Umar and V. E. Oberacker, Phys. Rev. C **74**, 061601 (2006).
[59] V. E. Oberacker, A. S. Umar, J. A. Maruhn, and P.-G. Reinhard, Phys. Rev. C **82**, 034603 (2010).
[60] A. S. Umar, V. E. Oberacker, J. A. Maruhn, and P.-G. Reinhard, Phys. Rev. C **80**, 041601 (2009).
[61] X. Jiang, J. A. Maruhn, and S. W. Yan, Eur. Phys. Lett. **112**, 12001 (2015).
[62] A. S. Umar and V. E. Oberacker, Phys. Rev. C **73**, 054607 (2006).
[63] E. Chabanat, P. Bonche, P. Haensel, J. Meyer, and R. Schaeffer, Nucl. Phys. A **635**, 231 (1998).
[64] A. S. Umar, M. R. Strayer, J. S. Wu, D. J. Dean, and M. C. Güçlü, Phys. Rev. C **44**, 2512 (1991).
[65] R. Keser, A. S. Umar, and V. E. Oberacker, Phys. Rev. C **85**, 044606 (2012).
[66] Kouhei Washiyama and Denis Lacroix, Phys. Rev. C **78**, 024610 (2008).
[67] V. E. Oberacker and A. S. Umar, Phys. Rev. C **87**, 034611 (2013).